*Supplementary Information for*

# Self-assembly and optical properties of porphyrin-based amphiphile

Ruijiao Dong,[a] Yang Bo,[b] Gangsheng Tong,[b] Yongfeng Zhou,[a] Xinyuan Zhu*[a] and Yunfeng Lu*[a,c]

[a] *School of Chemistry and Chemical Engineering, State Key Laboratory of Metal Matrix Composites, Shanghai Jiao Tong University, 800 Dongchuan Road, Shanghai 200240, P. R. China*

[b] *Instrumental Analysis Center, Shanghai Jiao Tong University, 800 Dongchuan Road, Shanghai 200240, P. R. China*

[c] *Department of Chemical and Biomolecular Engineering, University of California, Los Angeles, California 90095, United States*

* To whom correspondence should be addressed. Tel.: +86-21-34203400; E-mail: *xyzhu@sjtu.edu.cn*; *luucla@ucla.edu*

# *Contents*

**1. Materials**

**2. Instruments and Measurements**

**3. Synthesis Details**

**4. Self-Assemblies of Porphyrin-Based Nanoparticles**

**5. Supplemented Figures**

**6. References**

## 1. Materials

Pyridine-4-carboxaldehyde (97%, Alfa Aesar), pyrrole (≧98%, Alfa Aesar), propanoic acid (PPA) (99%, Shanghai Sinopharm Chemical Reagent Co. Ltd.), iodoethane (99%, Shanghai Aladdin Reagent Co. Ltd.), were used as received. 4-Bromomethyl azobenzene was synthesized according to the reported synthesis procedure,[1] and the detailed characterization data of this monomer was presented in our previous work.[2] $\alpha$-Cyclodextrin ($\alpha$-CD) (Shanghai Sinopharm Chemical Reagent Co. Ltd.) was dried for 48 h at 60 $^{o}$C in vacuum oven before use. Dimethyl formamide (DMF) from Shanghai Sinopharm Chemical Reagent Co. Ltd. was treated with calcium hydride ($CaH_2$) and distilled before use. Dimethyl sulphoxide (DMSO), methanol (MeOH), ethanol (EtOH), acetone, diethyl ether from Shanghai Sinopharm Chemical Reagent Co., Ltd, and distilled water were used as received.

## 2. Instruments and Measurements

### **Nuclear Magnetic Resonance** (NMR)

One-dimensional $^{1}$H-NMR spectra of the samples were recorded on a Varian Mercury plus 400 NMR spectrometer (400 MHz) with deuterated chloroform ($CDCl_3$), deuterated dimethyl sulfoxide (DMSO-$d_6$) and DMSO-$d_6$/deuterium oxide ($D_2O$) ($v$/$v$, 1/1) as solvents at 293 K. The chemical shifts were referenced to residual peaks of deuterated solvents: DMSO-$d_6$ (2.48 ppm), $D_2O$ (4.80 ppm), $CDCl_3$ (7.26 ppm).

### **Ultra Performance Liquid & Quadrupole-Time-of-Flight Mass Spectrometer (UMS)** (UPLC & Q-TOF-MS)

UPLC & Q-TOF-MS spectra of the products (TPyP, TEtPyP and TAzoPyP) were collected on a Waters-ACQUITY$^{TM}$ UPLC & Q-TOF-MS Premier (Waters Corporation, USA) at room temperature with methanol as the solvent. After being separated through UPLC columns, the samples were then analyzed by using Q-TOF-MS.

## **Fourier Transform Infrared Spectra** (FTIR)

FTIR spectra of the products (TPyP, TEtPyP and TAzoPyP) were recorded on a Paragon 1000 instrument by using the KBr sample holder method. The samples were firstly dried for 30 min to eliminate the residual moisture before measurement.

## **Dynamic Light Scattering** (DLS)

DLS measurement was performed on a Malvern Zetasizer NanoS apparatus equipped with a 4.0 mW laser operating at the wavelength of 633 nm. All sample solutions were measured at a scattering angle of 90$^{o}$ at 25 $^{o}$C. Before testing, the sample solution was filtered to get rid of dust by using some absorbent cotton. The concentration of sample solutions was 0.5 mg/mL. The sample solution was placed in the cell for at least 10 min prior to the measurement to allow for thermal equilibration.

## **Atomic Force Microscopy** (AFM)

The morphology of TAzoPyP monomer in different solvents and TAzoPyP/$\alpha$-CD complex in water was visualized using an atomic force microscopy (AFM) system with the Dimension 3100 model with a Nanoscope IIIa controller (Veeco, Santa Barbara, CA). The sample solutions with a concentration of approximate 0.1 mg/mL were dropped onto freshly cleaved mica sheets for 5 min, and then the excess solution was removed with a piece of filter paper. After a subsequent air-drying in the dark for 48 h, the samples were kept in the dark for AFM measurement. The samples were imaged using the tapping mode with setting of 256×256 pixels. Image analysis was performed using Nanoscope software after removing the background slope by flatting images.

## **Transmission Electron Microscopy** (TEM)

TEM measurement was carried out on a JEOL JEM-100CX-II instrument at a voltage of 200 kV. The specimens were prepared by directly drop-casting the sample

solution onto a carbon-coated copper grid and then air-drying at room temperature for 48 h before measurement.

## **Ultraviolet-Visible Absorption Spectra** (UV-Vis)

The UV-Vis absorption spectra of the sample solutions were obtained on a Thermo Electron-EV300 UV-Vis spectrophotometer at room temperature. The slit-width was set as 1 nm, and scan speed was set as 480 nm/min.

## **Steady-State Fluorescence Emission Spectra**

The fluorescence emission spectra were collected at room temperature on a PTI-QM/TM/IM steady-state & time-resolved fluorescence spectrofluorometer, made by USA/CAN Photon Technology International Int.. The excitation wavelength of the sample solutions was set at 360 nm or 415 nm for TAzoPyP as well as 394 nm for TPP. The slit-width was set as 2 nm or 4 nm, and the scan speed was set as 480 nm/min. The sample solutions were maintained in the fluorescence cuvette for 10 min prior to the measurement to allow for thermal equilibration.

## **Time-Resolved Fluorescence Spectra**

By using the time-correlated single-photon counting (TCSPC) technique, the time-resolved fluorescence spectra were recorded on a PTI-QM/TM/IM steady-state & time-resolved fluorescence spectrofluorometer, made by USA/CAN Photon technology international Int.. Utilizing the picosecond pulses from a doubled frequency, the time-resolved fluorescence spectra of the sample solutions with the excitation wavelength of 415 nm were detected at an emission wavelength of 655 nm for TAzoPyP in DMSO or MeOH and 700 nm for TAzoPyP or TAzoPyP/$\alpha$-CD in water for lifetime measurements with an emission polarizer and depolarizer.

## Zeta Potential Measurement

The zeta potentials ($\zeta$) of TAzoPyP or TAzoPyP/$\alpha$-CD complex in PBS buffer (pH = 7.4) were measured on a Malvern Zetasizer NanoS at 25 $^{o}$C. The cuvette was filled with the sample solution, and the measurement was performed in the $\zeta$-model for a minimum of 10 cycles and a maximum of 100 cycles.

## Circular Dichroism Spectra (CD)

CD spectra of TAzoPyP in different solvents were taken on a JASCO J-815 spectropolarimeter fitted with DRCD apparatus from 200 nm to 500 nm at room temperature.

## Wide-angle X-ray diffraction (WAXD)

WAXD was performed on a D/max-2200/PC diffractometer at room temperature, made by Japan Rigaku Corporation (Cu K$\alpha$ radiation $\lambda$ = 0.154 nm, $U$ = 40 kV, $I$ = 100 mA). The XRD patterns for all samples were collected in $2\theta$ range of 3$^{o}$–50$^{o}$. The samples were prepared by directly casting the sample solution onto a clean glass slide and then air-drying at room temperature for 48 h to form a sample film.

# 3. Synthesis Details

## 3.1 Synthesis of 5,10,15,20-tetra-(4-pyridyl)-porphyrin (TPyP)

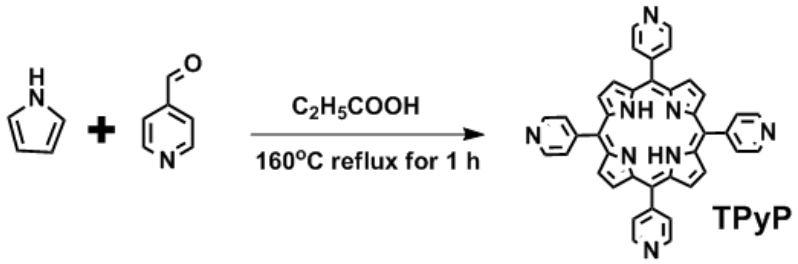


**Scheme S1** Synthesis route of TPyP.

According to previous literature,[3] pyridine-4-carboxaldehyde (15.0 g, 140 mmol) was dissolved in propionic acid (300 mL), pyrrole (9.4 g, 140 mmol) was added, and the mixture was refluxed for 1 h in the dark. The solvent was evaporated and the residue was dried under a vacuum. The crude product was taken in DMF (100 mL) and filtered. The product was washed with DMF (2×50 mL) and diethyl ether (2×50 mL) and dried under a vacuum at 80 °C. Yield: 2.75 g, purple solid (4.45 mmol, 19.2%).

**$^1$H-NMR** ($CDCl_3$, 400 MHz) (**Fig. S1**): $\delta_H$ (ppm) = -2.94 (s, -N*H*- on porphyrin group, 2H), 8.12-8.23 (m, -C*H*=CH-N= on Py-group, 8H), 8.87 (s, -C*H*=C*H*- on porphyrin group, 8H), 9.03-9.12 (m, =C*H*-N=C*H*- (close to N) on Py-group, 8H). **UPLC & Q-TOF-MS** of TPyP (**Fig. S2**): calculated for $[C_{40}H_{26}N_8+H]^+$: 619.2280, found m/z: 619.2365 $[M+H]^+$. **FTIR** (KBr) (**Fig. S3**): $\nu$ ($cm^{-1}$) = 536, 663, 726, 796 (C-H), 879, 973, 1072 (C-N), 1218, 1353, 1402, 1468, 1549, 1591 (C=C), 1664 (C=N), 2375, 3026, 3090, 3309/3419 (N-H).

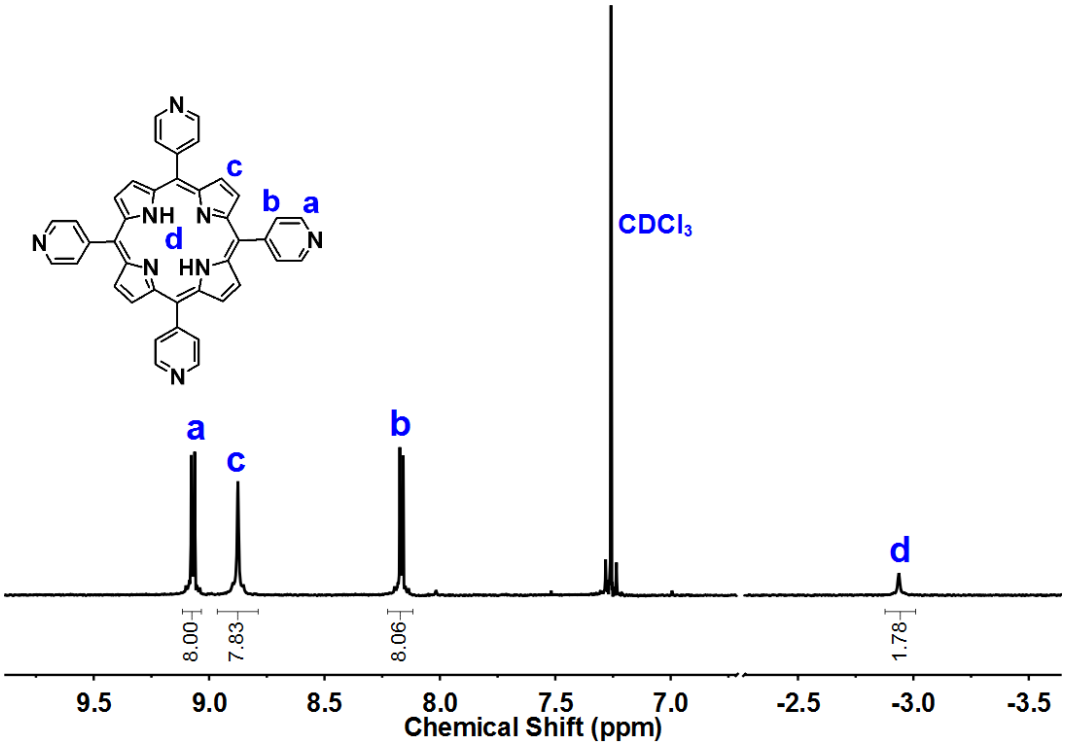


**Fig. S1** $^{1}$H-NMR spectrum of TPyP in $CDCl_3$.

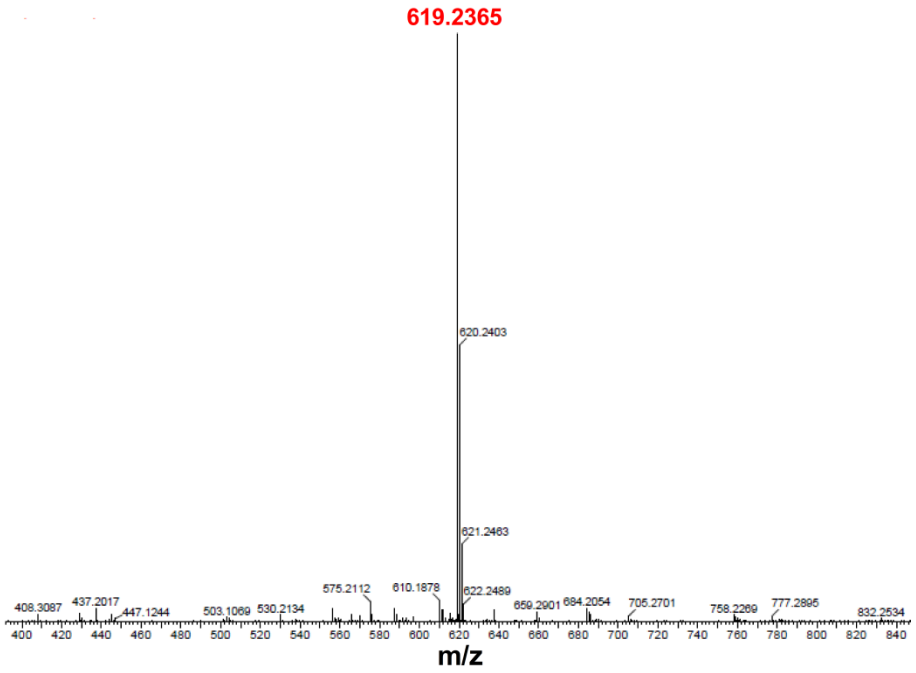


**Fig. S2** UPLC & Q-TOF-MS spectrum of TPyP.

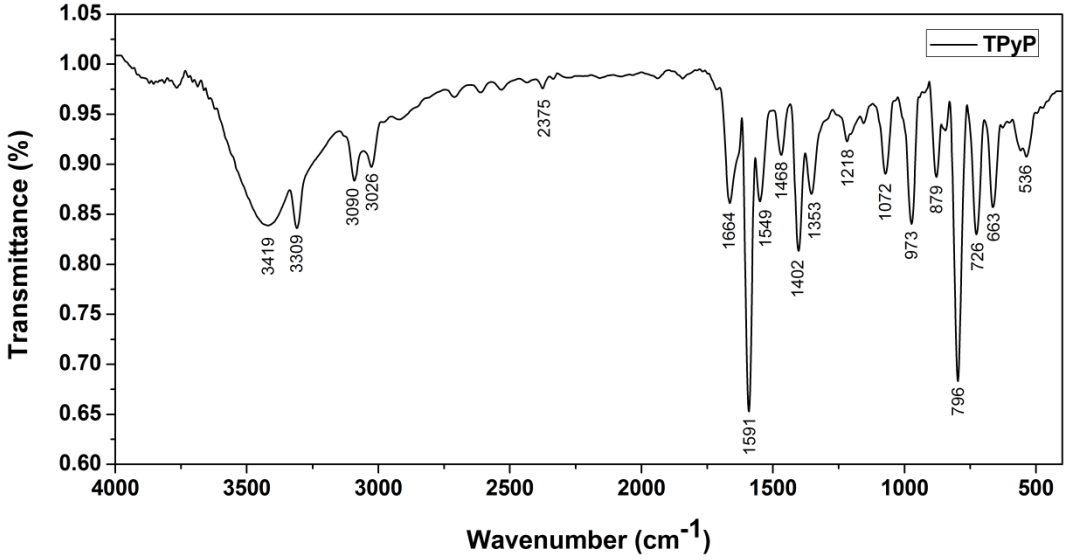


**Fig. S3** FTIR spectrum of TPyP.

## 3.2 Synthesis of 5,10,15,20-tetra-(4-*N*-ethylpyridyl)-porphyrin tetraiodide (TEtPyP)

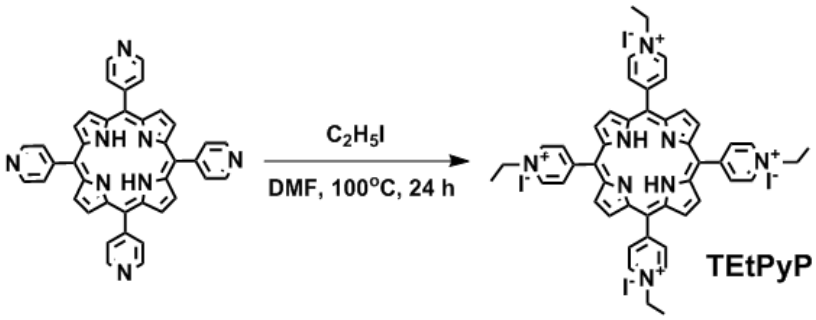


**Scheme S2** Synthesis route of TEtPyP.

The synthesis procedure of TEtPyP is conducted as follows. TPyP (0.337 g, 0.545 mmol) was dissolved in DMF (60 mL) and excess iodoethane (6.4 mL, 80 mmol) was added. The resulting solution was heated at 100 °C for 24 h. After being cooled to room temperature, acetone (100 mL) was added into the solution, and the formed precipitate was filtrated off, washed with diethyl ether and acetone for three times, collected and dried at 80 °C in vacuum to yield a brown powder (1.13 g, 0.91 mmol, 91%).

**$^1$H-NMR** (DMSO-$d_6$, 400 MHz) (**Fig. S4**): $\delta_H$ (ppm) = -3.10 (s, N*H* on porphyrin group, 2H), 1.90 (t, $J$ = 7.3 Hz, -$CH_2CH_3$, 12H), 5.01 (d, $J$ = 7.2 Hz, -$CH_2CH_3$, 8H), 9.01 (d, $J$ = 6.4 Hz, -C*H*=CH-N$^+$= on Py-group, 8H), 9.24 (s, -C*H*=C*H*- on porphyrin group, 8H), 9.58 (d, $J$ = 6.4 Hz, =C*H*-N$^+$=C*H*- (close to N$^+$) on Py-group, 8H). **UPLC & Q-TOF-MS** of TEtPyP (minus four iodine anions) (**Fig. S5**): calculated for $[C_{48}H_{46}N_8]^{2+}$: 367.1911 or $[C_{48}H_{46}N_8]^{3+}$: 244.7941, found m/z: 367.1840 $[M]^{2+}$ or 244.7873 $[M]^{3+}$. **FTIR** (KBr) (**Fig. S6**): $\nu$ (cm$^{-1}$) = 525, 720, 802, 872, 972, 1085, 1165 (C-N), 1225, 1352, 1393, 1452 (C-H on ethyl), 1510, 1558 (C=C), 1633 (C=N$^+$), 2375, 3026, 3318/3423 (N-H). **UV-Vis** (MeOH) (**Fig. S7**): $\lambda_A$ (nm) = 425 (Soret band of porphyrin), 516/552/591 (Q band of porphyrin).

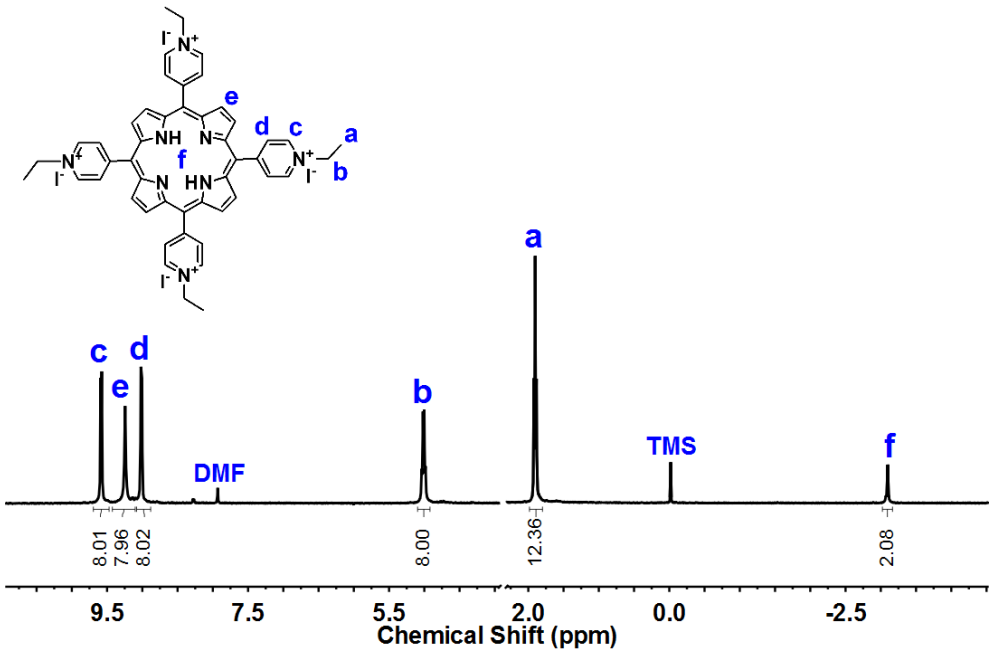


**Fig. S4** $^1$H-NMR spectrum of TEtPyP in DMSO-$d_6$.

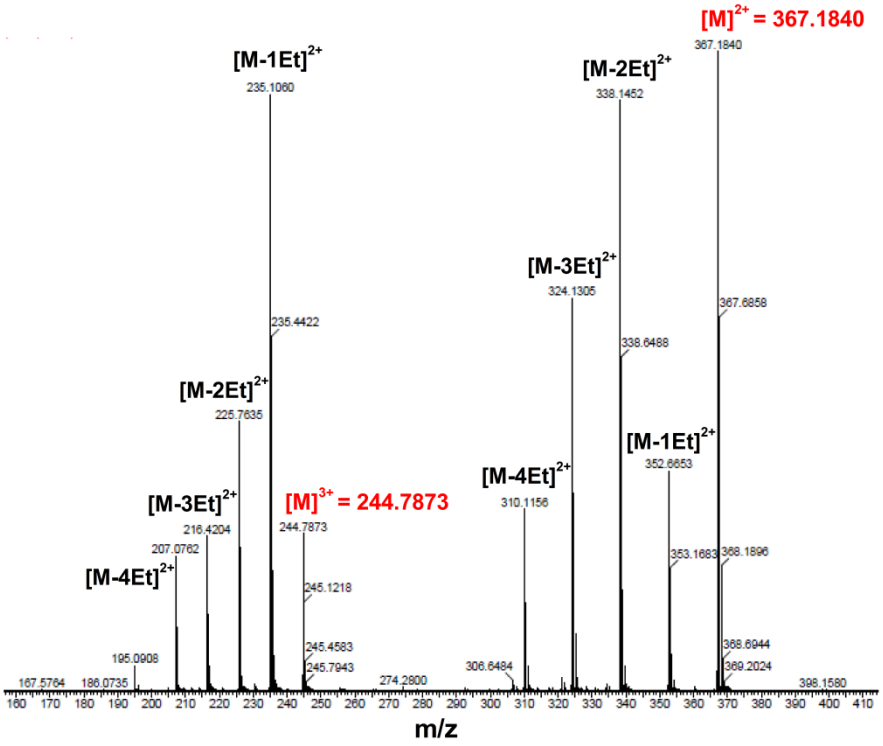


**Fig. S5** UPLC & Q-TOF-MS spectrum of TEtPyP.

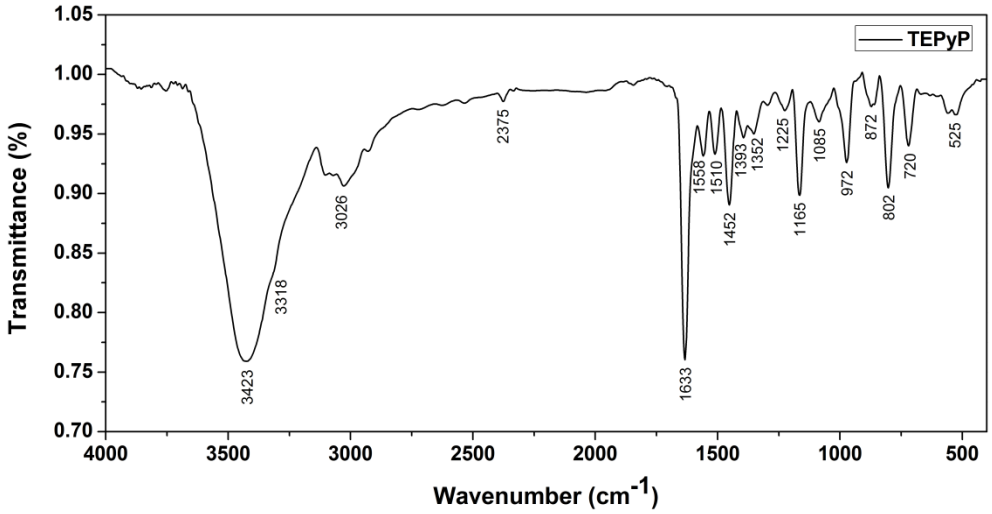


**Fig. S6** FTIR spectrum of TEtPyP.

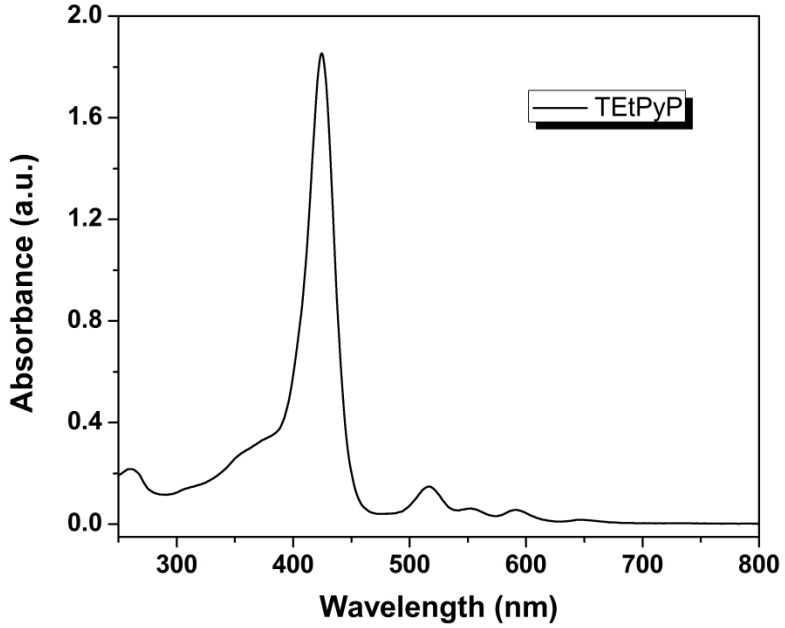


**Fig. S7** UV-Vis spectrum of TEtPyP in MeOH. The concentration of sample solutions was $1\times10^{-5}$ M.

## 3.3 Synthesis of 5,10,15,20-tetra-(4-*N*-methyl-azobenzene-pyridyl)-porphyrin tetrabromide (TAzoPyP)

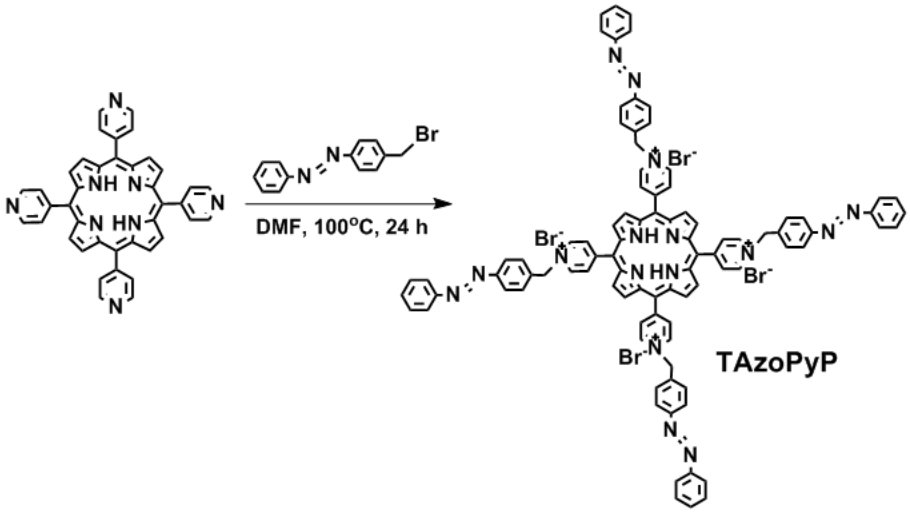


**Scheme S3** Synthesis route of TAzoPyP.

A solution of Azo-Br (1.2 g, 4.36 mmol) and TPyP (0.337 g, 0.545 mmol) in 50 mL

DMF was allowed to react at 100 °C for 24 h. After being cooled to room temperature, the formed precipitate was filtrated and washed with ethyl ether and acetone for three times, collected and dried at 80 °C in vacuum to yield a brown powder (0.825 g, 0.48 mmol, 88.05%).

**$^1$H-NMR** (DMSO-$d_6$, 400 MHz) (**Fig. S8**): $\delta_H$ (ppm) = -3.10 (s, N*H* on porphyrin group, 2H), 6.35 (s, $N^+$(Py)-C$H_2$-Ph, 8H), 7.63 (m, *H* on Azo group, 12H), 7.95 (m, *H* on Azo group, 8H), 8.12 (s, *H* on Azo group, 16H), 9.07 (d, $J$ = 6.43, -C*H*=CH-$N^+$= on Py-group, 8H), 9.24 (s, -C*H*=C*H*- on porphyrin group, 8H), 9.73 (d, $J$ = 6.40, =C*H*-$N^+$=C*H*- (close to $N^+$) on Py-group, 8H). **UPLC & Q-TOF-MS** of TAzoPyP (minus four bromide anions) (**Fig. S9**): calculated for $[C_{92}H_{70}N_{16}]^{2+}$: 699.2982, found m/z: 699.2883 $[M]^{2+}$. **FTIR** (KBr) (**Fig. S10**): $\nu$ ($cm^{-1}$) = 552, 640, 689, 721, 799, 852, 972, 1008, 1155 (C-N), 1211, 1293, 1402, 1450 (C-H on ethyl), 1508, 1558 (C=C), 1632 (C=$N^+$), 2375, 3038, 3316/3416 (N-H). **UV-Vis** (MeOH) (**Fig. S11**): $\lambda_A$ (nm) = 322 (π-π* transition of *trans*-Azo), 429 (Soret band of porphyrin), 519/554/592 (Q band of porphyrin).

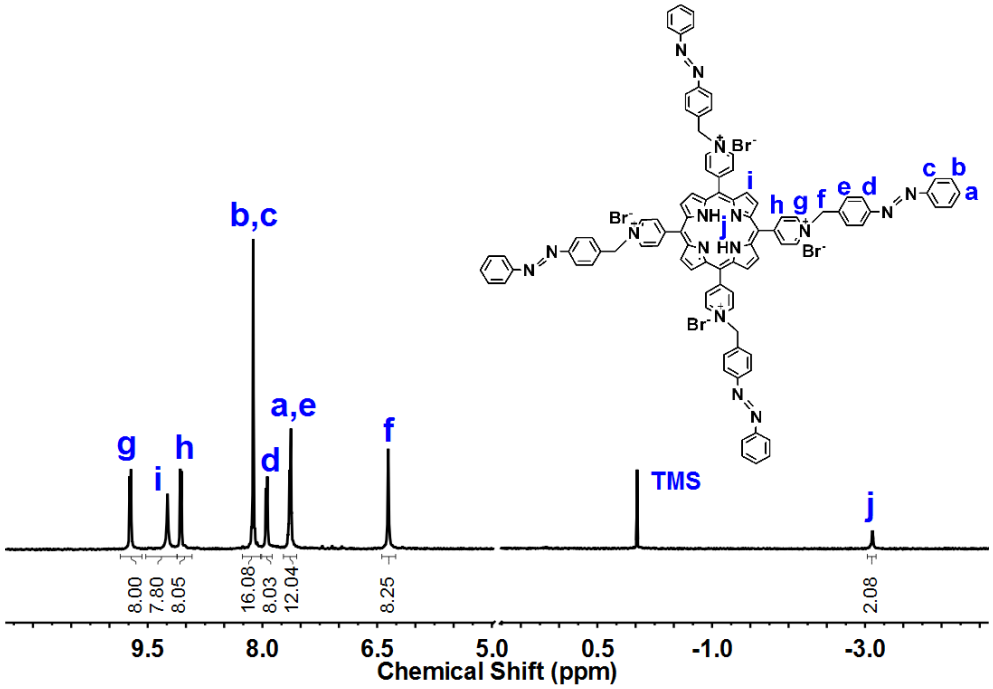

**Fig. S8** $^{1}$H-NMR spectrum of TAzoPyP in DMSO-$d_6$.

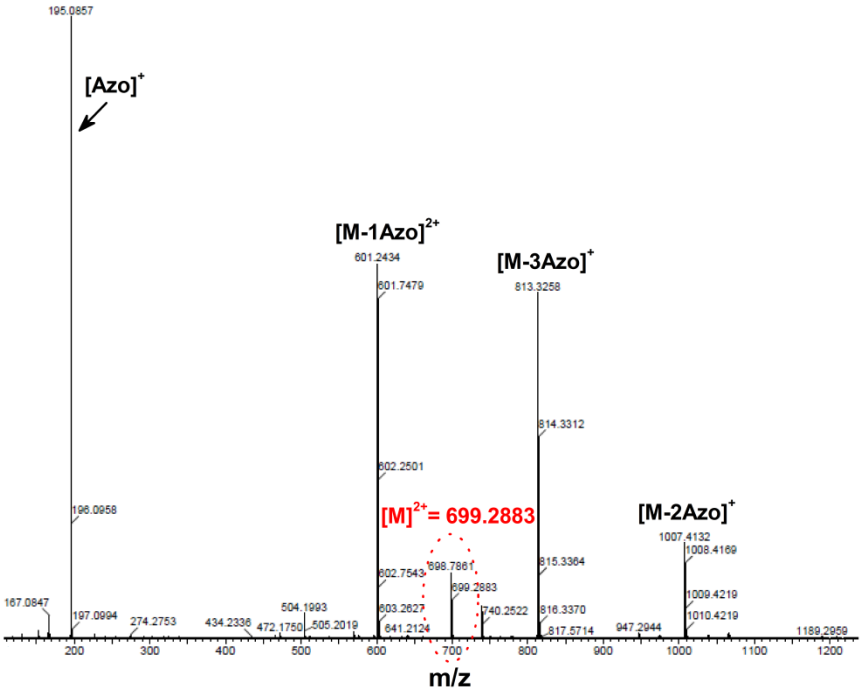


**Fig. S9** UPLC & Q-TOF-MS spectrum of TAzoPyP.

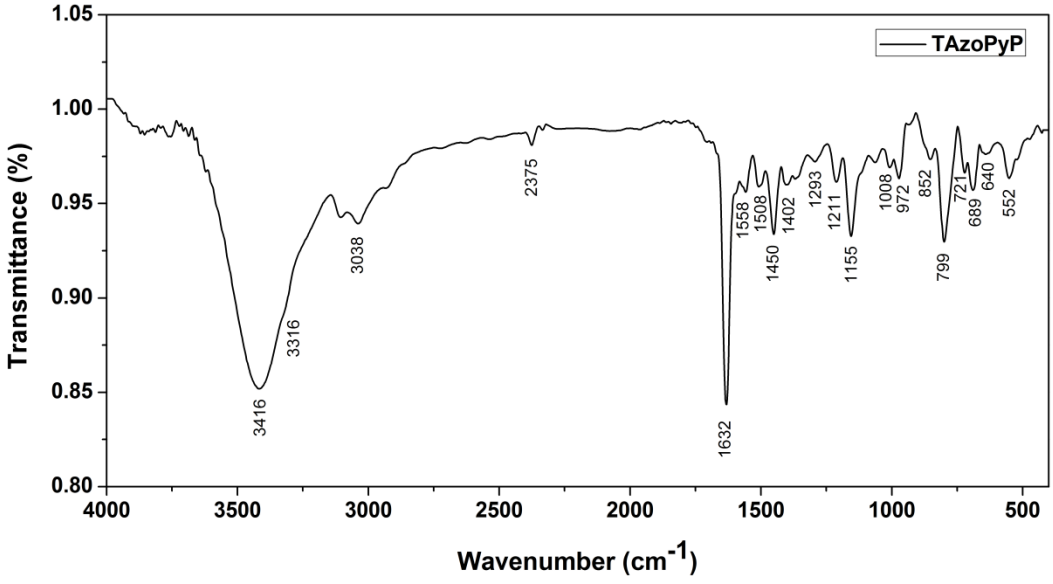


**Fig. S10** FTIR spectrum of TAzoPyP.

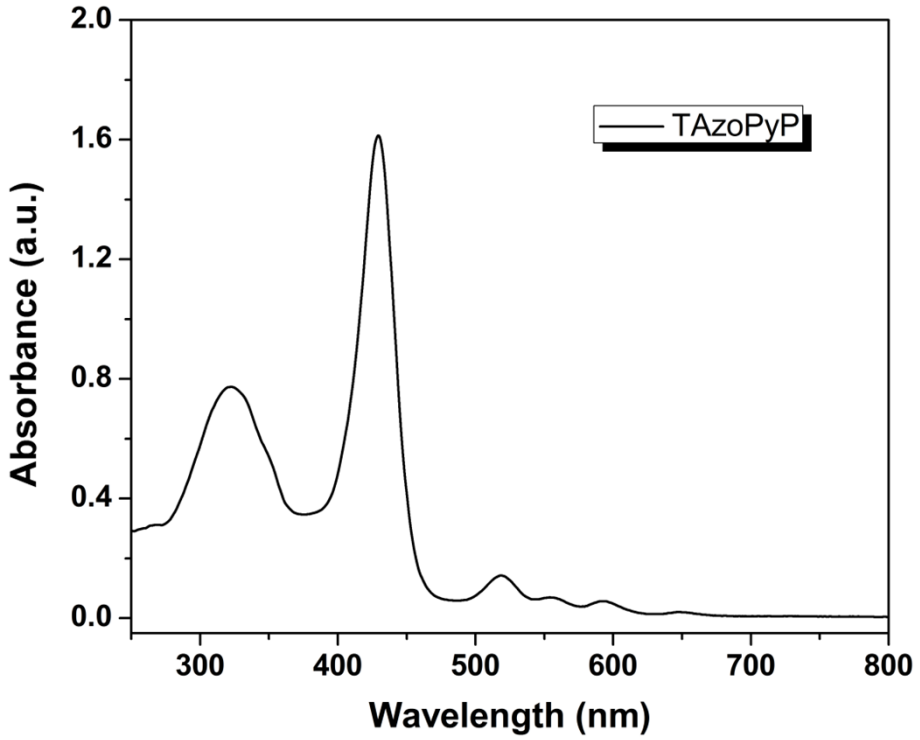


**Fig. S11** UV-Vis spectrum of TAzoPyP in MeOH. The concentration of sample solutions was $1\times10^{-5}$ M.

## 4. Self-Assemblies of Porphyrin-Based Nanoparticles

### A) Self-assembly of TAzoPyP nanopartciles

The TAzoPyP nanoparticles were prepared according to the following procedures: 2 mL of DMSO solution containing 10 mg TAzoPyP was slowly added dropwise via a syringe pump into 10 mL of deionized water for about 2 h under vigorous stirring. Then, the resulting solution was left at room temperature with constant stirring for another 2 h after the addition was completed. Subsequently, the self-assembled solution enclosed in a dialysis membrane (MWCO = 2.0 kDa), was dialyzed against deionized water for 48 h to remove DMF. Finally, the volume of the resulting aqueous solution was then made up to 20 mL to obtain an aggregate solution with a concentration of 0.5 mg/mL for further experiments. **Notes:** The above experimental procedures were carried out in the dark.

### B) Self-assembly of TAzoPyP/*α*-CD supramolecular nanopartciles

The supramolecular nanoparticles were prepared according to the following procedures: 10 mg of TAzoPyP (1 equiv.) and 24 mg of *α*-CD (4 equiv.) were firstly dissolved in 2 mL DMSO with continuous stirring for 6 h to obtain TAzoPyP/*α*-$CD_4$ complex. The above solution was then added dropwise via a syringe pump into 10 mL of deionized water for about 2 h under vigorous stirring. After stirring another 2 h, the resulting solution was followed by dialysis in a dialysis membrane (MWCO = 2.0 kDa) against deionized water for 48 h to remove DMF. Finally, the volume of the resulting aqueous solution was increased to 20 mL to obtain an aggregate solution with a concentration of 0.5 mg/mL (for TAzoPyP only) for further experiments. **Notes:** The above experimental procedures were carried out in the dark.

## 5. Supplemented Figures

### 5.1. Determination of association constant for Azo/*α*-CD system

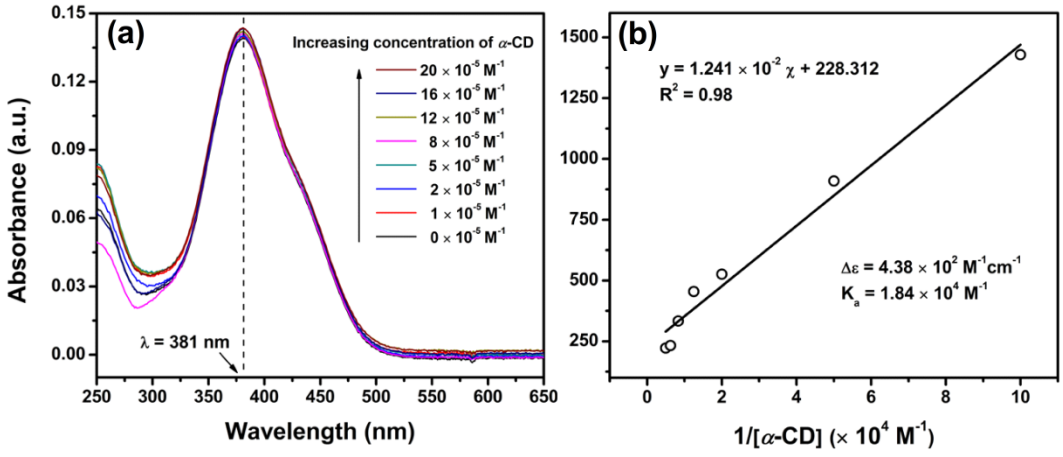


**Fig.. S12** The UV absorption of azobenzene upon stepwise addition excess *α*-CD in MeOH/$H_2O$ (*v*/*v*, 1/1). The concentration of azobenzene was $1\times10^{-5}$ M.

As shown in **Fig. S12**, the association constant between azobenzene and *α*-CD in MeOH/$H_2O$ (*v*/*v*, 1/1) was determined by following the UV absorptions at 381 nm. The

concentration of azobenzene was set at $1\times10^{-5}$ M. With the addition of *α*-CD, the absorption of azobenzene gradually enhanced. Since *α*-CD can exactly form a 1:1 inclusion complex with azobenzene, the inclusion complexation of *α*-CD (**H**) with azobenzene (**G**) is expressed by the following equations, respectively:

$$\mathbf{H} + \mathbf{G} \overset{K_a}{\leftrightarrow} \mathbf{H} \cdot \mathbf{G}$$

We employed the usual double reciprocal plot according to the modified Hidebrand-Benesi equation:

$$\frac{\mathbf{1}}{\Delta \boldsymbol{A}} = \frac{\mathbf{1}}{\boldsymbol{K_a}\Delta\boldsymbol{\varepsilon}[\mathbf{H}][\mathbf{G}]} + \frac{\mathbf{1}}{\Delta\boldsymbol{\varepsilon}[\mathbf{G}]}$$

Where **H**, **G**, $\boldsymbol{K_a}$ represents guest (azobenzene), host (*α*-CD) and association constant, respectively. $\boldsymbol{\Delta A}$ denotes the absorbance difference before and after host molecules are added. $\boldsymbol{\Delta\varepsilon}$, which denotes the difference of the molar extinction coefficient between the host and host-guest complex at the same wavelength, is $4.38\times10^{2}$ $M^{-1}cm^{-1}$ for Azo/*α*-CD system. The association constant $\boldsymbol{K_a}$ is calculated by the equation:

$$\boldsymbol{K_a} = \frac{\boldsymbol{b}}{\boldsymbol{k}} = \mathbf{1.84 \times 10^4\ M^{-1}}$$

Where $\boldsymbol{k}$ is the slope value of the line plot, and $\boldsymbol{b}$ is the intercept of the line plot.

## 5.2. TEM image of TAzoPyP/α-CD supramolecular nanoparticles

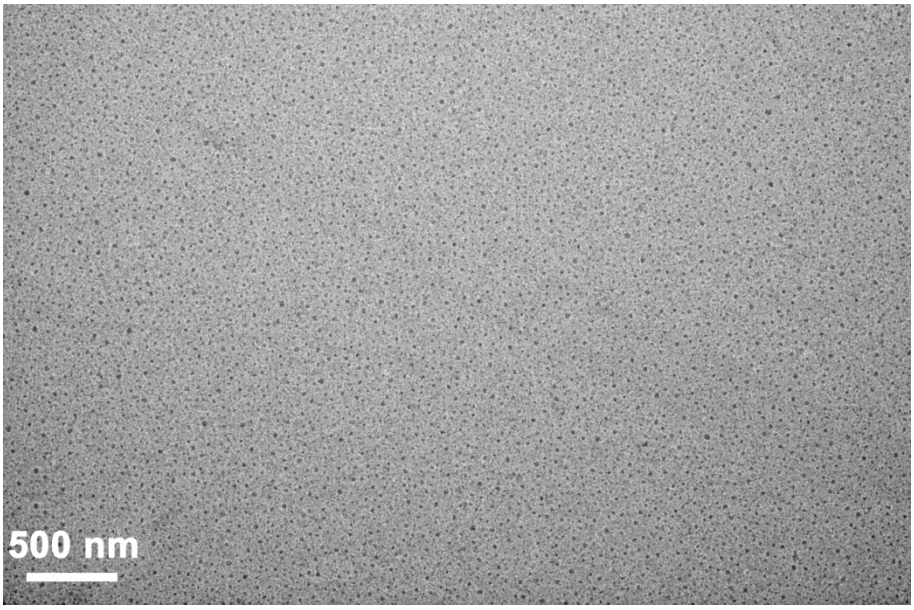


**Fig. S13** Large-scale TEM image of TAzoPyP/α-CD supramolecular nanoparticles.

According to the TEM observation in **Fig. S13**, the TAzoPyP/α-CD supramolecular complex in water exhibits well-defined spherical nanoparticles with uniform size and dispersion. The statistic size of the obtained supramolecular nanoparticles based on the TEM image is approximately 35 nm, which is in good agreement with the hydrodynamic diameter of 46±1.4 nm determined by DLS.

## 5.3. Determination of zeta potentials of TAzoPyP-based nanoparticles

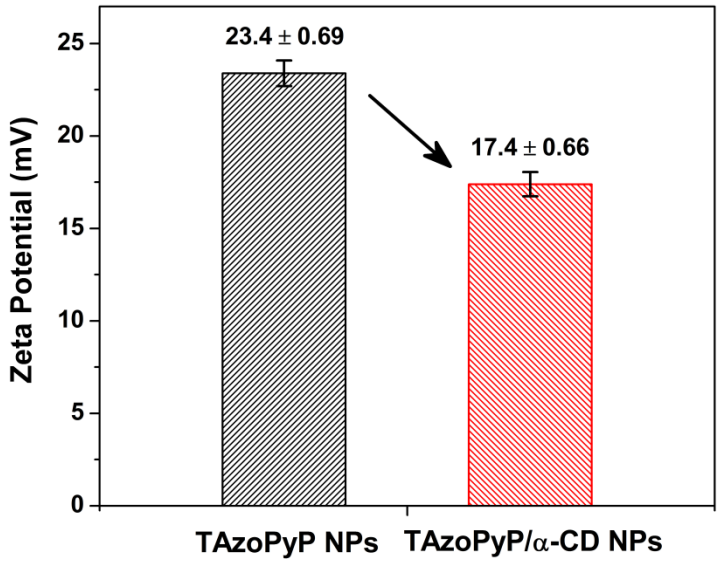


**Fig. S14** Zeta potentials of TAzoPyP nanoparticles and TAzoPyP/α-CD supramolecular nanoparticles in PBS buffer (pH = 7.4) with the same TAzoPyP concentration of 0.1 mg/mL.

## 5.4. UV-Vis spectra of TEtPyP in different solvents

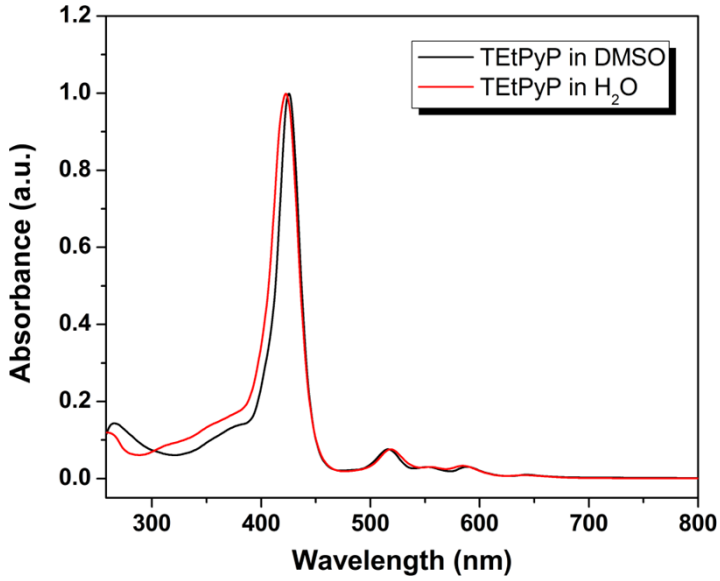


**Fig. S15** Normalized UV-Vis spectra of TEtPyP in DMSO and $H_2O$ at room temperature.

As shown in **Fig. S15**, the UV-Vis spectrum of TEtPyP in DMSO is characterized by two main absorption bands for the Soret band of the porphyrin chromophore at *ca.* 425 nm along with the Q band of the porphyrin chromophore from 500 to 650 nm. We found that no apparent aggregates could be observed when TEtPyP was dissolved in DMSO, suggesting that TEtPyP remains predominantly unimolecular in DMSO. In addition, the UV adsorption band (Soret band of the porphyrin) of TEtPyP in water shows a slight blue shift compared with that in the good solvent of DMSO, indicating that TEtPyP adopts a H-type aggregation in the aqueous medium. Since this blue shift of the Soret band of the porphyrin chromophore is relatively small, it implies that the intermolecular π-π stacking interaction of TEtPyP in water is very weak due to its high water-solublity.

## 5.5. Molecular Model of TAzoPyP

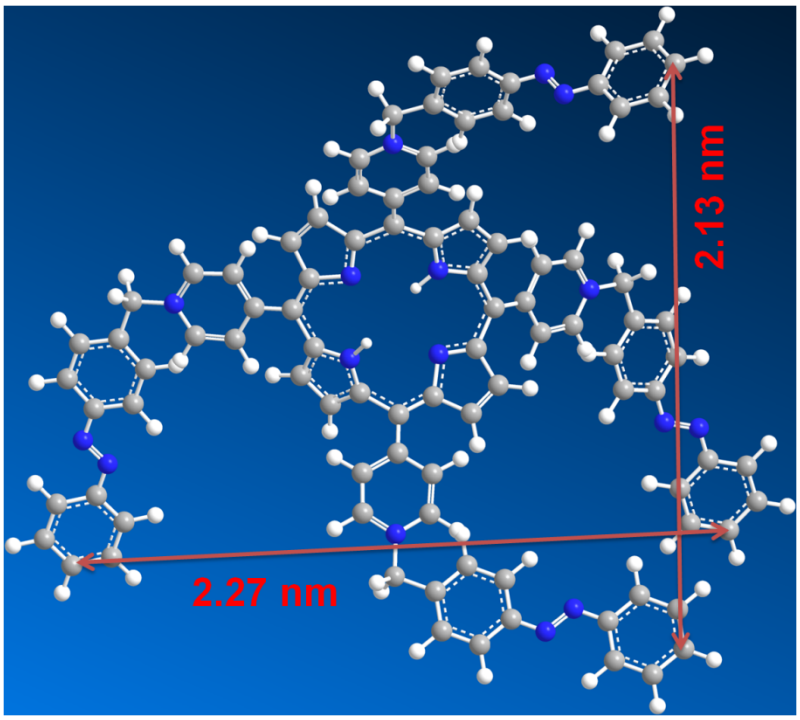


**Fig. S16** Molecular model of TAzoPyP and its molecular size according to the ***Chem 3D*** results.

## 5.6. XRD analyses for TAzoPyP and the resulting aggregates

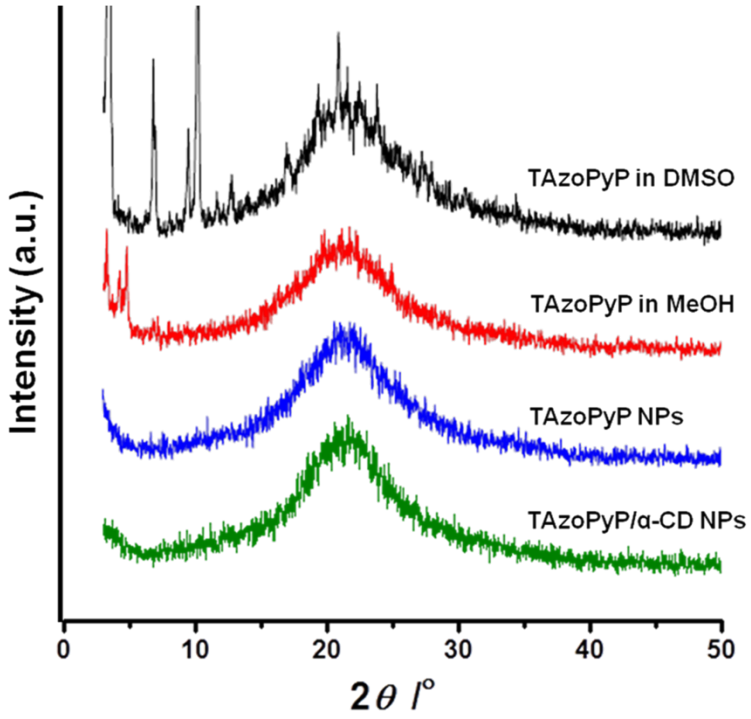


**Fig. S17** XRD patterns of TAzoPyP in DMSO, TAzoPyP in MeOH, TAzoPyP NPs and TAzoPyP/α-CD NPs in $2\theta$ range of 0°–50°. All samples were measured at room temperature.

In order to get more insight into the phase in the material, wide-angle XRD was performed for these TAzoPyP-based systems. In **Fig. S17**, the wide-angle XRD profile for TAzoPyP in DMSO shows not only a broad peak at wide angle around 20.88°, but also several sharp peaks at small angle ($2\theta$ = 3.4°, 6.8° and 10.2°), indicating that the crystal exists in the casting film from unimolecular TAzoPyP. For TAzoPyP nanosheets in MeOH, its wide-angle XRD pattern also shows a broad peak at wide angle around 20.88° and a sharp peak at small angle 4.78°. The peak at $2\theta$ = 4.78° is a first-order diffraction and indicates a lamellar structure, which is consistent with the results of AFM, TEM and UV-Vis analyses. However, these wide-angle XRD patterns for TAzoPyP NPs

and TAzoPyP/α-CD NPs only exhibit a broad peak at wide angle around 20.88° and no sharp peak can be observed at small angle, suggesting that no crystal exists in these spherical nanoparticles. It might be concluded that the disordered stacking of TAzoPyP molecules in these nanoparticles greatly restricts the formation of crystal.

## 5.7. Donor-acceptor pairs between azobenzene and porphyrin in TAzoPyP

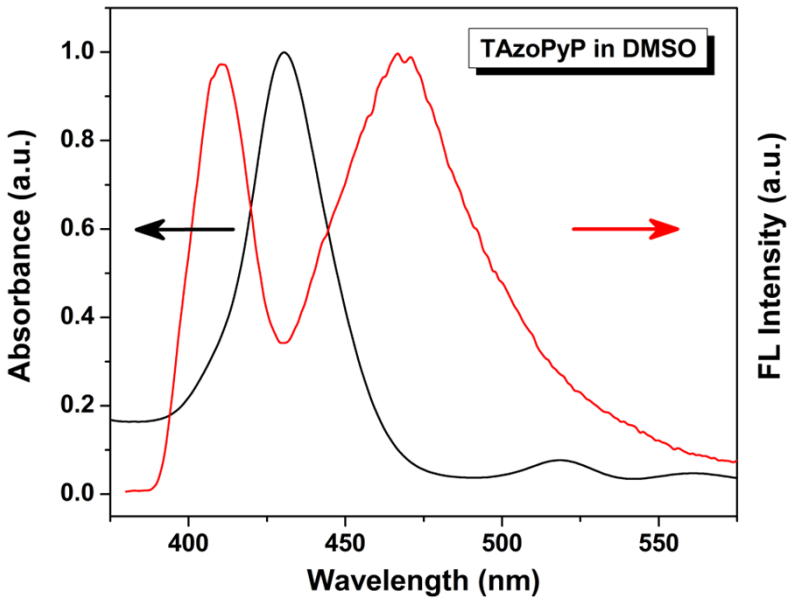


**Fig. S18** The partial normalized UV-Vis absorption spectrum (black line) of porphyrin moiety of TAzoPyP in DMSO and partial normalized fluorescence spectrum (red line) of the azobenzene group of TAzoPyP in DMSO excited with an excitation wavelength of 360 nm.

In **Fig. S18**, the fluorescence emission peaks of the azobenzene group of TAzoPyP overlap the absorption band of the porphyrin moiety of TAzoPyP perfectly, making it possible for the porphyrin moiety to absorb the fluorescence emitted by the azobenzene group through fluorescence resonance energy transfer (FRET). Therefore, the azobenzene and porphyrin can be used as a new donor-acceptor pair for FRET in this system.

## 5.8. Fluorescence excitation spectra of TAzoPyP in MeOH

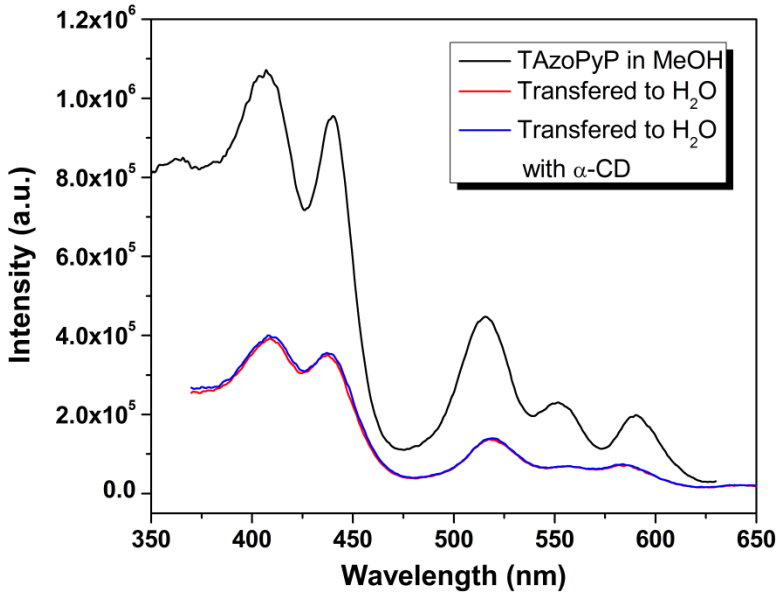


**Fig. S19** Fluorescence excitation spectra of TAzoPyP in MeOH as well as its resulting aggregates dispersed in $H_2O$ with an excitation wavelength of 415 nm at room temperature. The concentration of the sample solutions was set as $1\times10^{-5}$ M.

In **Fig. S19**, the appearance of a new excitation peak at *ca.* 440 nm demonstrates the formation of a large number of aggregates for TAzoPyP in MeOH. When the resulting lamellar aggregates were transferred from MeOH to the aqueous medium, the intermolecular π-π stacking interactions of TAzoPyP in water further led to the formation of a heirachical π-stacking aggregates. Accordingly, a weakening and broadening excitation peak can be observed. In addition, it was found that the addition of α-CD into the resulting aqueous solution hardly affected the aggregation behavior of TAzoPyP lamellar structures.

## 5.9. Fluorescence emission spectra of TAzoPyP in MeOH

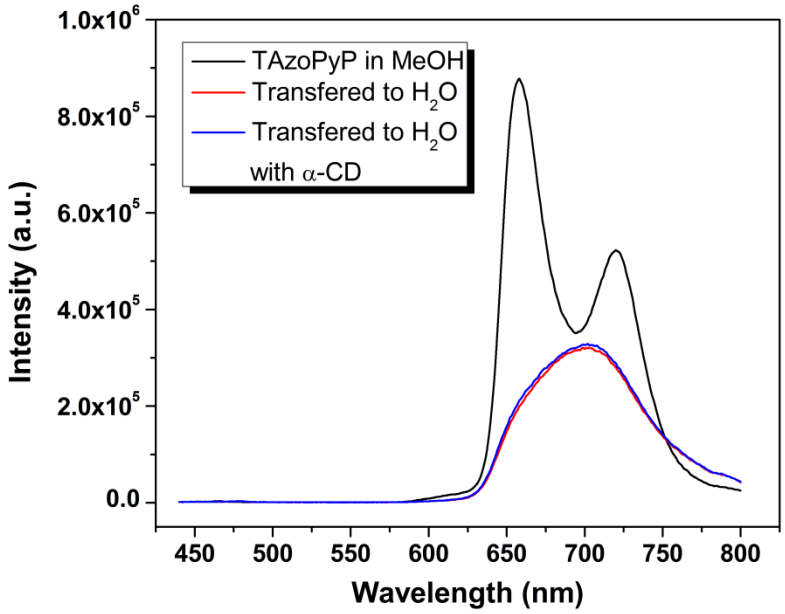


**Fig. S20** Fluorescence emission spectra of TAzoPyP in MeOH as well as its resulting aggregates dispersed in $H_2O$ with an excitation wavelength of 415 nm at room temperature. The concentration of sample solutions was $1\times10^{-5}$ M.

In **Fig. S20**, the steady-state fluorescence spectrum of TAzoPyP in MeOH upon direct excitation of the porphyrin moiety at 415 nm just presents two diagnostic fluorescence emission bands for the porphyrin moiety at 650 and 715 nm, while only a single fluorescence emission peak can be observed for the aqueous solution of the lamellar aggregates dispersed in water. In contrast to TAzoPyP in MeOH, the lamellar aggregates dispersed in water show a fluorescence band red-shifting in position and decreasing in intensity, which is mainly caused by the intermolecular π-π stacking interaction of TAzoPyP in water. Besides, the addition of α-CD has little effect on the fluorescent behavior of the aqueous solution of the lamellar aggregates.

## 5.10. Fluorescence excitation/emission spectra of TPP in THF

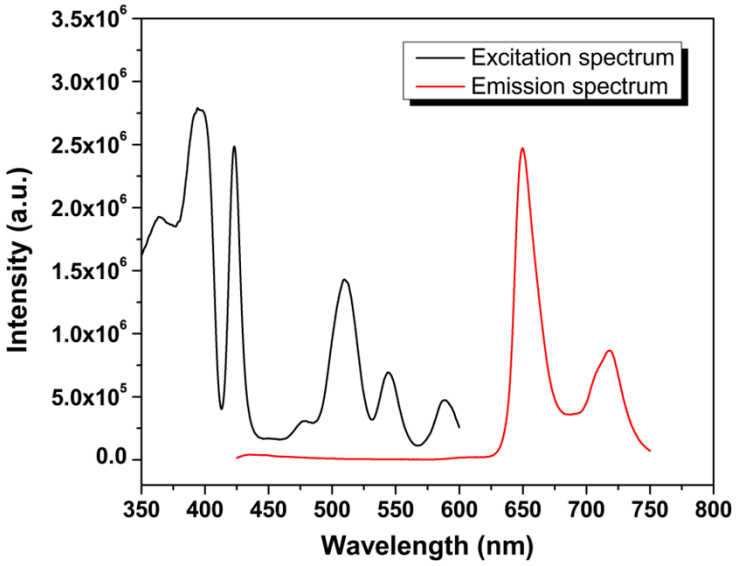


**Fig. S21** Fluorescence excitation/emission spectra of TPP in THF excited at 394 nm at room temperature. The concentration of sample solutions was $1\times10^{-5}$ M.

## 5.11. Fluorescence lifetime of TPP in THF

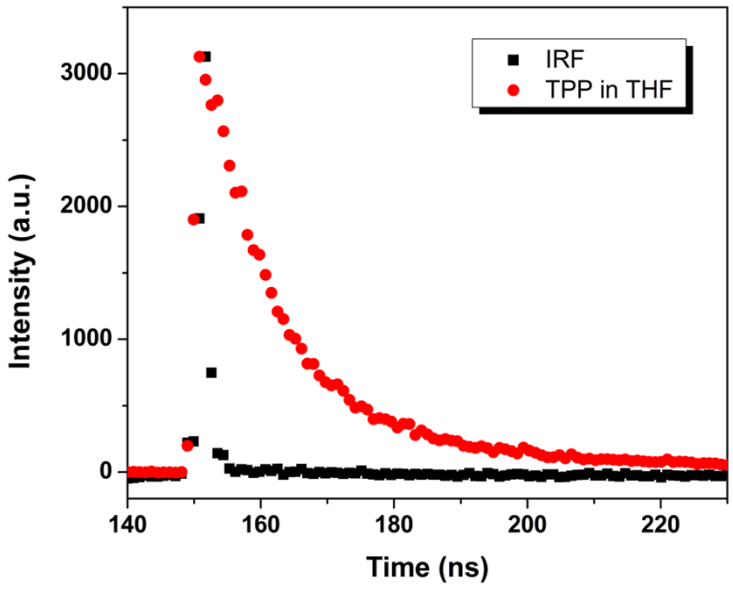


**Fig. S22** Time-resolved fluorescence spectrum of TPP in THF with an excitation wavelength of 394 nm. The concentration of sample solutions was $1\times10^{-5}$ M.

As a control, the time resolved fluorescence spectrum of the THF solution of TPP has been given in **Fig. S22**. Furthermore, TPP in THF with 394 nm excitation yields a decay best fit to a single exponential decay with a long lifetime ($\tau_{Fl}$) component of 12.15 ns, which is very close to the lifetime value of 13.2 ns for TPP in toluene.[4]

## 5.12. TAzoPyP in DMSO by photo-irradiation

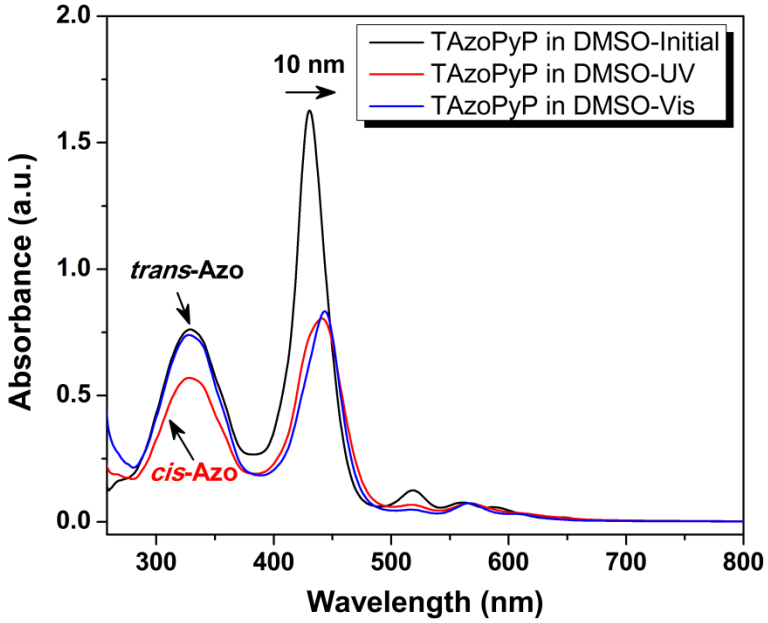


**Fig. S23** UV-Vis spectra of TAzoPyP in DMSO at the initial state, after UV-365 irradiation for 5 min and after Vis-450 irradiation for 10 min. The concentration of the sample solutions was 10 μM.

In **Fig. S23**, when the DMSO solution of TAzoPyP was irradiated by UV light for 5 min, a significant decrease in the absorption intensity for the azobenzene group at *ca.* 324 nm can be observed, which is indicative of the photoisomerization of azobenzene from the *trans*-form to the *cis*-form. Meanwhile, the absorption peak for the porphyrin is greatly reduced, which implies that the photobleaching behavior of porphyrin occurrs.[5] Furthermore, by irradiation with Vis light at 450 nm for 10 min, the absorption band for

the azobenzene group at *ca.* 324 nm reverts back to the its initial intensity, indicating that the azobenzene group of TAzoPyP undergoes a reversible photoisomerization from the *cis*-form to the *trans*-form. In addition, the porphyrin moiety of TAzoPyP exhibits an irreversible photobleaching upon alternating irradiation with UV and Vis light.

## 5.13. TAzoPyP in MeOH by photo-irradiation

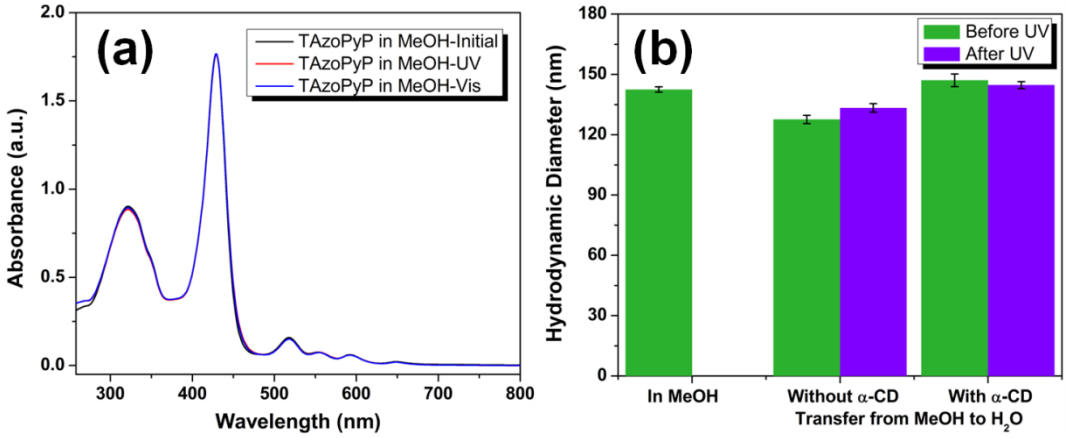


**Fig. S24** (a) UV-Vis spectra of TAzoPyP in MeOH ($c$ = 10 μM) at the initial state, after UV-365 irradiation for 5 min and after Vis-450 irradiation for 10 min. (b) The hydrodynamic diameter variation of the aggregates for TAzoPyP in MeOH by UV-365 or Vis-450 irradiation.

In **Fig. S24a**, the absorption intensity of TAzoPyP in MeOH remains constant upon alternating UV and Vis irradiation, which indicates that the TAzoPyP nanosheets in MeOH could hardly respond to UV and Vis light illumination. The photoisomerization of azobenzene group and photobleaching of porphyrin moiety have been greatly suppressed by the intermolecular π-π stacking interaction of TAzoPyP in MeOH. As shown in **Fig. S24b**, we monitored the change in size of the lamellar aggregates dispersed in water before and after UV irradiation by using the DLS. The hydrodynamic diameter of the lamellar aggregates still remains constant at around 130 nm after UV irradiation. In addition, the addition of α-CD slightly affects the photostability of the lamellar

aggregates.

## 5.14. TEtPyP in DMSO and $H_2O$ by photo-irradiation

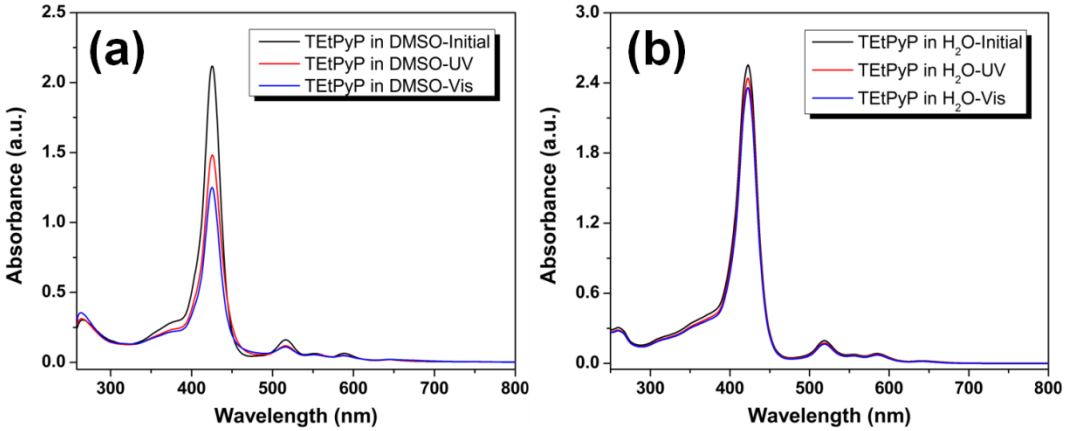


**Fig. S25** UV-Vis spectra of (a) TEtPyP in DMSO and (b) TEtPyP in $H_2O$ ($c$ = 10 μM) at the initial state, after UV-365 irradiation for 5 min and after Vis-450 irradiation for 10 min.

As shown in **Fig. S25a**, the absorption band (e.g., Soret band) of TEtPyP in DMSO greatly decreases under UV and Vis irradiation, suggesting that the TEtPyP in DMSO can respond mechanically to light illumination. In contrast, TEtPyP in water exhibits high photostability, so that the absorption intensity of TEtPyP in water yet remains constant upon alternating UV and Vis irradiation (**Fig. S25b**).

## 6. References

[1] Z. Liu and M. Jiang, *J. Mater. Chem.*, 2007, **17**, 4249–4254.

[2] R. J. Dong, Y. Liu, Y. F. Zhou, D. Y. Yan and X. Y. Zhu, *Polym. Chem.*, 2011, **2**, 2771–2274.

[3] S. Sugata, S. Yamanouchi and Y. Matsushima, *Chem. Pharm. Bull.*, 1977, **25**, 884–889.

[4] J.-P. Strachan, S. Gentemann, J. Seth, W. A. Kalsbeck, J. S. Lindsey, D. Holten and D.

F. Bocian, *J. Am. Chem. Soc.*, 1997, **119**, 11191–11201.

[5] (*a*) J. D. Spikes, *Photochem Photobiol.*, 1984, **39**, 797–808; (*b*) T. S. Mang, T. J. Dougherty, W. R. Potter, D. G. Boyle, S. Somer and J. Moan, *Photochem Photobiol.*, 1987, **45**, 501–506; (*c*) R. Bonnett, B. D. Djelal, P. A. Hamilton, G. Martinez and F. Wierrani, *J. Photochem. Photobiol. B*, 1999, **53**, 136–143.